Supplement of Atmos. Chem. Phys., 15, 11081–11096, 2015
http://www.atmos-chem-phys.net/15/11081/2015/
doi:10.5194/acp-15-11081-2015-supplement

Atmospheric Chemistry and Physics
Open Access

Supplement of

VOC species and emission inventory from vehicles and their SOA formation potentials estimation in Shanghai, China

C. Huang et al.

Correspondence to: C. Huang (huangc@saes.sh.cn)

1. Measured VOC species of different vehicle types and gas evaporation

Table S1 lists the weight percentage of individual VOC from different vehicle types and gas evaporation. The top 5 major species from LDGV were m,p-xylene, toluene, o-xylene, ethylbenzene, and n-decane, occupying 7.5%, 7.4%, 5.5%, 4.3%, and 3.9% of the total VOC, respectively. The top 5 major species from taxi were toluene, m,p-xylene, o-xylene, ethylbenzene, and 1,2,4-trimethylbenzene, occupying 7.7%, 5.9%, 4.9%, 4.5%, and 3.5% of the total VOC, respectively. The top 5 major species from HDDT were n-dodecane, n-undecane, propene, acetone, and n-decane, occupying 11.4%, 9.8%, 9.8%, 7.5%, and 6.6% of the total VOC, respectively. The top 5 major species from bus were n-dodecane, propene, n-undecane, n-decane, and acetone, occupying 15.9%, 11.9%, 7.6%, 7.1%, and 6.5% of the total VOC, respectively. 2-methylhexane, m,p-xylene, ethylbenzene, o-xylene, and methyl-tertbutyl-ether were major species in the exhaust of motorcycle, which contributed 23.4%, 9.3%, 5.5%, 4.4%, and 4.0% of the total VOC. Propane, isopentane, isobutene, 1-pentene, and n-butane were major species of gas evaporation, contributing 15.99%, 11.87%, 9.69%, 8.87%, and 6.51% of the total VOCs, respectively.

Table S1. Weight percentage (wt.%) of individual VOC from different vehicle types and gas evaporation.

VOC species	LDGV	Taxi	HDDT	Bus	Motorcycle	Gas evaporation
Ethane	0.45±0.07	0.41±0.03	0.82±0.51	0.46±0.15	2.88±1.20	ND
Propane	0.03±0.03	0.04±0.02	2.35±1.55	1.26±1.19	1.09±0.75	19.59±2.68
n-butane	0.53±0.08	0.48±0.06	0.25±0.14	0.27±0.13	1.33±0.45	7.89±3.41
n-pentane	2.31±0.23	2.52±0.27	0.51±0.21	0.34±0.05	0.87±1.24	5.27±1.54
n-hexane	3.04±0.55	2.97±0.17	0.53±0.19	0.98±0.74	2.88±1.22	1.32±0.56
n-heptane	1.60±0.21	1.47±0.09	1.04±0.33	0.92±0.38	2.33±1.21	0.54±0.50
n-octance	2.51±0.31	3.06±1.11	1.69±0.62	1.20±1.08	0.58±0.30	ND
n-nonane	0.96±0.12	0.98±0.18	3.79±1.11	3.56±1.17	0.25±0.23	ND
n-decane	3.95±0.47	3.51±0.71	6.62±1.27	7.10±2.66	0.15±0.14	ND
n-undecane	0.38±0.08	0.52±0.41	9.78±3.27	7.60±0.44	0.06±0.10	ND
n-dodecane	0.16±0.02	0.29±0.07	11.36±2.61	15.94±11.44	0.06±0.09	ND
Isobutene	0.24±0.05	0.27±0.03	0.35±0.12	0.59±0.72	1.47±0.43	11.73±5.85
Isopentane	2.97±0.20	2.85±0.29	2.02±0.67	1.60±1.30	2.54±2.32	14.27±2.94

2,2-dimethylbutane	0.72±0.40	0.86±0.44	ND	ND	0.43±0.15	1.30±0.98
2,3-dimethylbutane	1.02±0.17	1.16±0.10	1.41±1.57	ND	1.29±0.48	0.60±0.18
2-methylpentane	2.27±0.15	1.9±0.31	0.52±0.33	ND	1.90±0.97	1.96±0.50
3-methylpentane	2.05±0.51	1.84±0.41	1.43±0.50	0.58±0.73	2.00±0.83	0.90±0.30
2-methylhexane	1.26±0.38	1.31±0.31	0.52±0.40	0.43±0.10	23.43±10.72	1.28±0.88
3-methylhexane	1.10±0.23	0.90±0.10	0.89±0.86	0.68±0.22	1.55±0.29	0.35±0.10
2,4-dimethylpentane	0.02±0.01	0.05±0.01	ND	0.35±0.26	0.61±0.30	0.13±0.16
2,3-dimethylpentane	1.02±0.32	0.68±0.08	0.61±0.41	0.18±0.00	1.36±0.51	0.06±0.07
2,3,4-trimethylpentane	0.11±0.04	0.16±0.02	ND	0.60±0.57	0.48±0.64	0.07±0.14
3-methylheptane	1.61±0.19	1.61±0.23	1.01±0.32	1.01±0.58	0.68±0.46	ND
2,2,4-trimethylpentane	1.39±0.52	1.03±0.17	1.04±0.67	0.60±0.01	0.91±0.85	0.87±0.88
2-methylheptane	1.96±0.18	1.96±0.23	1.00±0.24	1.04±0.90	0.55±0.31	ND
Cyclopentan	1.36±0.44	1.28±0.14	0.03±0.01	0.04±0.02	1.17±0.33	0.04±0.04
Cyclohexane	0.48±0.12	0.35±0.04	ND	ND	0.98±0.70	1.41±1.74
Methylcyclopentane	2.63±0.15	2.62±0.82	0.07±0.02	0.10±0.06	1.31±0.48	0.68±0.20
Methylcyclohexane	1.68±0.66	0.95±0.17	0.24±0.06	0.34±0.26	0.77±0.48	0.07±0.09
Ethene	0.40±0.08	0.37±0.05	0.75±0.47	0.43±0.13	3.13±1.49	2.94±2.07
Propene	1.18±0.68	1.92±0.34	9.78±1.33	11.92±0.18	0.79±0.42	2.05±0.15
1,3-butadiene	0.01±0.00	0.02±0.02	ND	ND	0.04±0.02	0.04±0.02
1-butene	2.05±0.25	2.03±0.34	1.17±0.61	0.88±0.10	1.76±0.65	3.90±1.09
trans-2-butene	0.19±0.13	0.24±0.05	0.24±0.10	0.22±0.08	0.40±0.53	3.64±0.84
cis-2-butene	0.27±0.01	0.86±1.27	0.15±0.06	0.16±0.06	0.54±0.36	1.79±0.72
isoprene	0.03±0.01	0.03±0.02	ND	ND	0.05±0.02	0.06±0.08
trans-2-pentene	0.95±0.24	0.53±0.07	0.16±0.11	0.13±0.01	0.36±0.22	0.64±0.09
cis-2-Pentene	0.38±0.18	0.76±0.13	0.08±0.04	0.07±0.00	0.27±0.27	2.68±0.22
1-pentene	0.35±0.12	0.27±0.02	1.10±0.77	0.72±0.02	0.65±0.33	10.13±2.77
1-hexene	0.74±0.21	1.26±0.59	1.78±1.51	1.32±0.27	1.59±0.98	1.10±0.59
Ethyne	0.40±0.05	0.36±0.02	0.74±0.46	0.42±0.15	2.54±1.23	ND
Benzene	2.90±0.53	2.88±0.33	3.37±0.75	2.92±0.55	1.34±0.33	0.09±0.02
Toluene	7.37±0.1	7.72±0.71	3.02±0.61	2.3±2.11	2.50±0.81	0.34±0.09
Styrene	2.09±0.23	2.21±0.31	0.12±0.02	0.24±0.13	0.23±0.10	0.01±0.01
Ethylbenzene	4.3±0.23	4.53±0.37	0.95±0.13	0.94±0.79	5.53±5.26	0.03±0.01
m,p-Xylene	7.53±0.56	5.88±0.52	2.13±0.33	2.44±0.78	9.34±6.48	0.02±0.02
o-Xylene	5.55±0.46	4.85±0.38	0.74±0.07	0.91±0.26	4.37±5.00	0.02±0.00
1,3,5-trimethylbenzene	1.82±0.07	1.91±0.31	0.35±0.06	0.45±0.14	0.55±0.49	0.01±0.01
1,2,4-trimethylbenzene	3.48±0.26	3.55±0.32	1.15±0.31	1.56±0.73	0.65±0.53	ND
isopropylbenzene	0.49±0.11	0.63±0.04	0.08±0.02	0.10±0.02	0.12±0.07	ND
n-propylbenzene	0.71±0.09	0.72±0.08	0.24±0.04	0.30±0.10	0.30±0.16	ND
m-ethyltoluene	0.49±0.19	0.57±0.15	0.55±0.24	0.93±0.44	0.37±0.32	ND
p-ethyltoluene	2.32±0.99	3.52±0.40	0.32±0.09	0.49±0.22	0.20±0.15	ND
o-ethyltoluene	1.15±0.34	1.49±0.37	0.20±0.14	0.20±0.07	0.31±0.23	ND
1,2,3-trimethylbenzene	1.77±0.24	2.11±0.43	0.73±0.15	1.04±0.43	0.29±0.3	ND

m-diethylbenzene	0.69±0.16	0.79±0.47	0.22±0.06	0.42±0.26	ND	ND
p-diethylbenzene	0.87±0.18	1.11±0.18	0.56±0.84	2.58±3.26	ND	ND
Acetone	0.63±0.12	0.42±0.07	7.53±4.57	6.47±1.26	0.55±0.54	ND
isopropanol	0.06±0.03	0.04±0.01	ND	1.09±1.17	0.01±0.01	ND
methyl-ethyl-ketone	0.05±0.01	0.05±0.03	1.83±1.24	1.42±0.64	ND	ND
Tetrahydrofuran	0.07±0.01	0.07±0.01	0.21±0.07	0.19±0.04	ND	ND
Vinylacetate	0.01±0.01	0.01±0.01	2.32±0.81	1.41±0.04	ND	ND
Dioxane	0.01±0.00	0.02±0.01	ND	ND	ND	ND
Ethylacetate	0.09±0.01	0.10±0.02	0.87±0.21	1.07±0.06	1.12±0.47	ND
Methyl-tertbutyl-ether	0.08±0.00	0.11±0.03	0.28±0.06	0.46±0.28	3.96±1.96	ND
4-methyl-2-pentanone	0.14±0.03	0.10±0.02	0.2±0.04	0.25±0.01	ND	ND
2-hexanone	0.03±0.02	0.10±0.02	0.55±0.21	0.39±0.11	ND	ND

2. Observation data of meteorological condition and air pollutant concentration

Fig. S1 shows the location of the monitoring site in this study. The site was on the roof of a 5-floor building (15 m high above the ground) at Shanghai Academy of Environmental Science (31.17ºN, 121.43ºE), which was located southwest of the urban area of Shanghai. The site was mostly surrounded by commercial properties and residential dwellings. Vehicle exhaust was a major source of pollutants near this site.

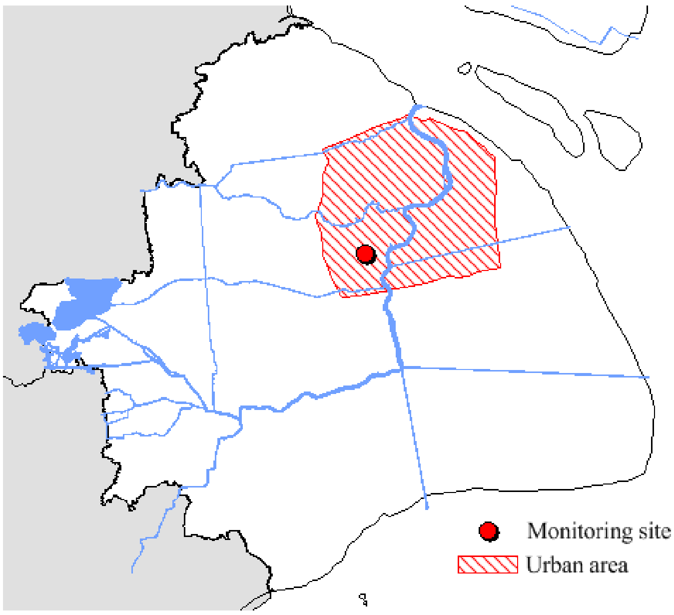

Fig. S1. Location of the monitoring site.

Fig. S2 shows time series observation data of meteorology parameters and CO, O_3, VOCs species, OC, and EC concentration in summer (from January 1 to January

31) and winter (from August 1 to August 31) in the atmosphere of Shanghai urban in 2013. Detail information of the monitoring site was introduced by Qiao et al. (2014). During the winter observation, air temperature varied in the range of -0.8-18.0°C and the average temperature was 5.5±3.8°C. Relative humidity (RH) fluctuated in the range of 23.3-84.9% and the average RH was 59.8±12.9%. Wind speed was in the range of 0.6-4.5$m \cdot s^{-1}$ and the average wind speed was 2.0±0.7$m \cdot s^{-1}$. The average concentrations of CO, ethylbenzene, and m,p-xylene in winter were 993±544ppb, 1.16±1.09ppb, and 1.27±1.11ppb. The maximum O_3 concentration was 74ppb. The average concentrations of OC and EC were 13.40±8.68$\mu g \cdot m^{-3}$ and 2.72±2.17$\mu g \cdot m^{-3}$.

During the summer observation, air temperature varied in the range of 23.7-43.0°C and the average temperature was 31.9±3.8°C. Relative humidity (RH) fluctuated in the range of 22.6-80.4% and the average RH was 58.2±12.8%. Wind speed was in the range of 0.6-5.4$m \cdot s^{-1}$ and the average wind speed was 1.2±0.8 $m \cdot s^{-1}$. The average concentrations of CO, ethylbenzene, and m,p-xylene in summer were 721±140ppb, 0.73±0.57ppb, and 0.26±0.21ppb. The maximum O_3 concentration was 164ppb. The average concentrations of OC and EC were 7.44±4.81$\mu g \cdot m^{-3}$ and 1.37±0.86$\mu g \cdot m^{-3}$.

Concentrations of CO, ethylbenzene, xylene, OC and EC showed good consistency in the observation period. The photochemical exposure ($\Delta t \cdot [OH]$) was calculated using Eq. (1). The figure indicates during the period with high ozone, the OC/EC ratio and $\Delta t \cdot [OH]$ is much higher than during the other periods. More secondary formation of OC can be expected during the high ozone period.

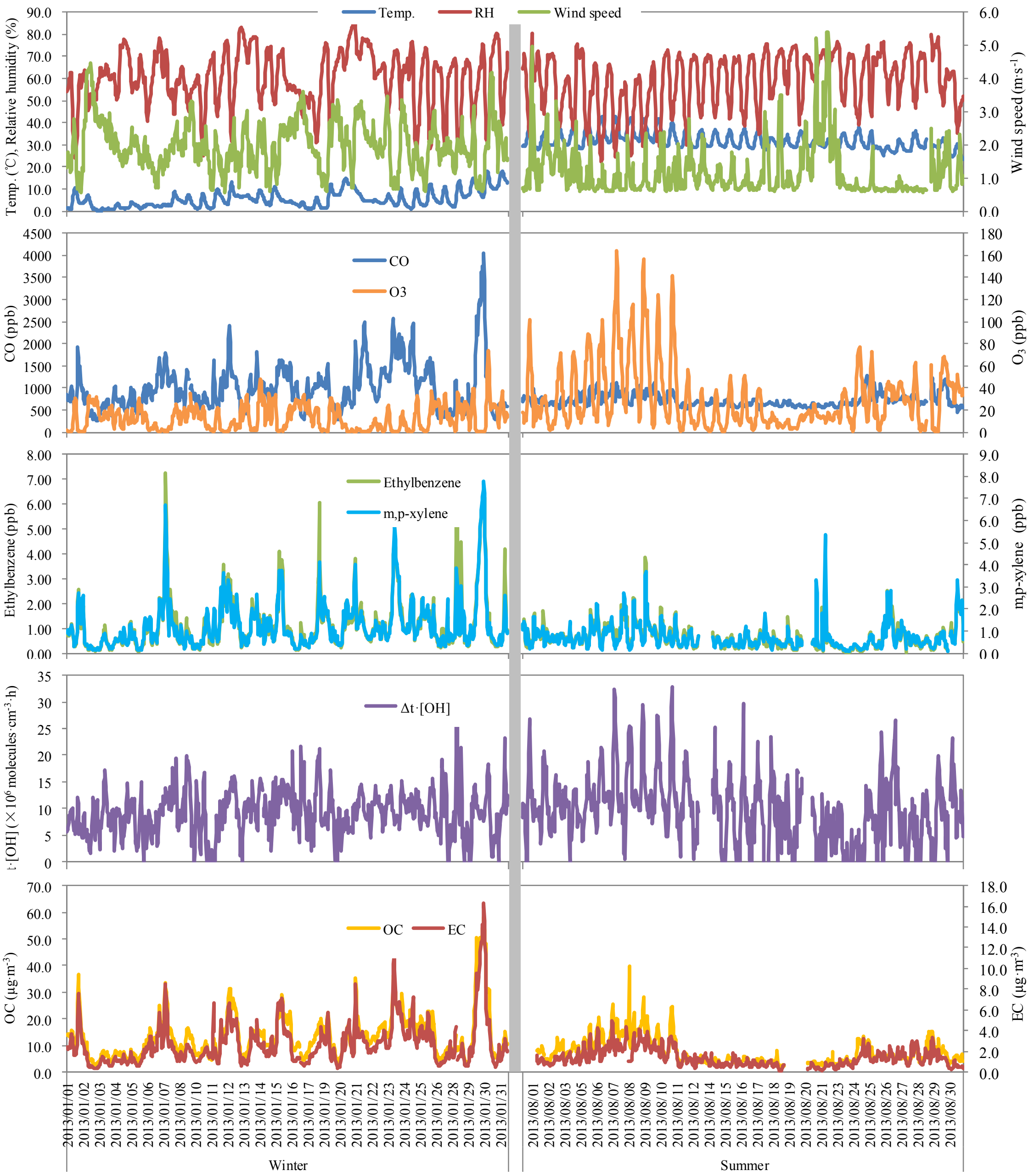

Fig. S2. Time series observation data of meteorological condition and CO, O_3, ethylbenzene, m,p-xylene, OC, and EC concentration in Shanghai urban in 2013.

3. Correlationship of ethylbenzene and m,p-xylene during the observation period

Fig. S3 shows the correlationship of hourly ethylbenzene and m,p-xylene concentration in the urban atmosphere during the observation period in Shanghai. It was indicated that these two species presented strong correlationship whether in summer or winter. The ratios of m,p-xylene to ethylbenzene were 1.09 and 1.04, and the correlation coefficients were 0.88 and 0.96 in summer and winter, respectively.

The correlationship implied that two species mainly came from the same source. According to the measured VOCs profiles from vehicle exhaust, vehicle emission could be the major source of m,p-xylene to ethylbenzene.

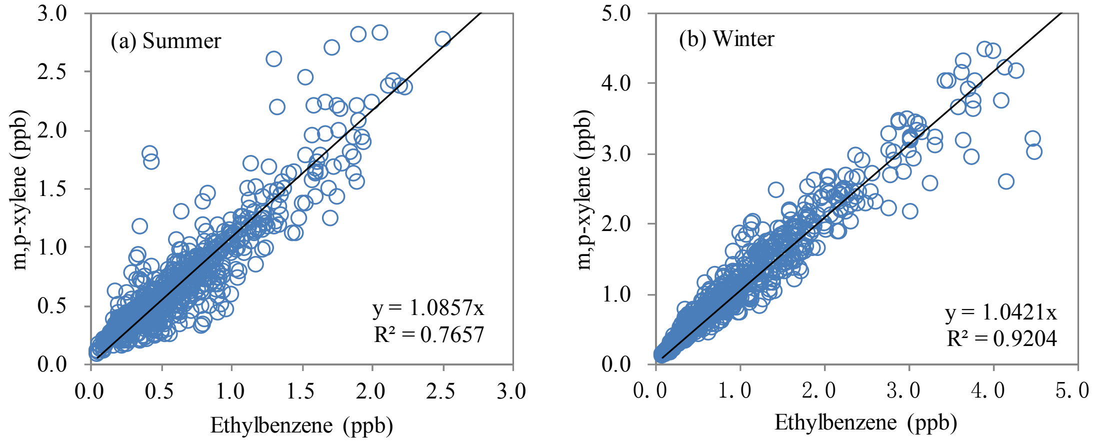

Fig. S3. Correlation between ethylbenzene and m,p-xylene mixing ratios in summer and winter in 2013.

Fig. S4 shows the diurnal distribution of average concentrations of ethylbenzene and m,p-xylene in summer and winter during the observation period. The average concentrations of ethylbenzene and m,p-xylene were normalized to 1 at 0:00 am. It was indicated that there was an obvious depletion of m,p-xylene compared with ethylbenzene in daytime. And more m,p-xylene depletion was observed in summer than in winter. On this account, we used the ratios of m,p-xylene to ethylbenzene to characterize the photochemical age.

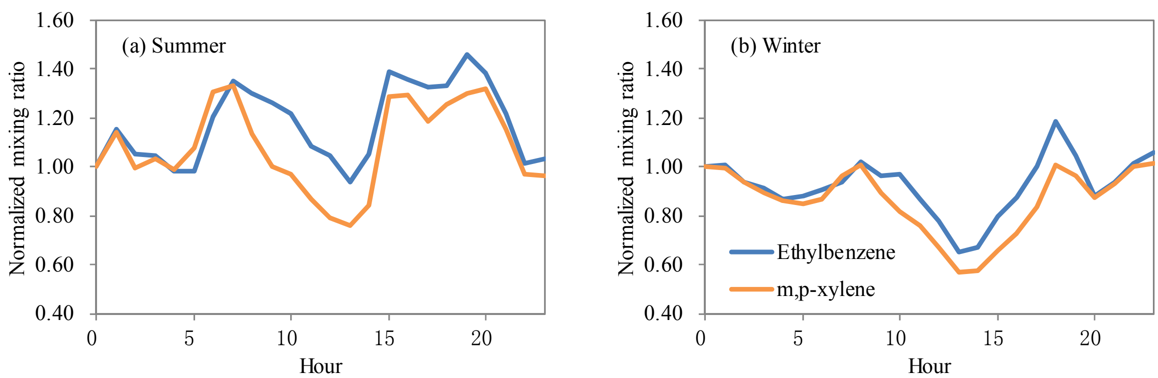

(a) Summer (b) Winter

Fig. S4. Diurnal distribution of average concentrations of ethylbenzene and m,p-xylene in summer and winter in 2013.

4. Vehicular CO emission contribution in Shanghai

Fig. S5(a) shows CO emission contribution of different sources in Shanghai in 2012. The methodology of CO emission inventory compilation has been introduced by Huang et al. (2011). The emission sources covered power plants, boilers, industrial processes including iron and steel manufacturing, oil refining, cement producing, etc., vehicles, off-road mobile sources, and residential fuel combustion. The activity data were updated to the year of 2012 from the pollution source census data, national key pollution source list, and statistical yearbook. Total CO emission amount was 1236.1 tons for the whole city of Shanghai in 2012. Iron & steel manufacturing was the major source of CO emission, which accounted for 55% of the total. The sector produced 19.7×10^6 and 18×10^6 tons of pig irons and crude steels, and consumed more than 10×10^6 tons of coal in 2012. Vehicle was the second major source, taking up 27.8% of the total CO emission.

Based on the emission inventory, we used CMAQ model to simulate the CO concentrations at the observation site during January and August in 2013. Two scenarios of with and without vehicular CO emission were simulated by using brute force method to distinguish the contribution of vehicular CO emission to the receptor. The meteorological data was from the results of the Weather Research and Forecasting Model (WRF). Fig. S5(b) shows the proportions of vehicle exhaust and other sources to CO concentration at the observation site. Fig. S6 shows the times series simulation data of CO concentration with the emission inventories of total sources and vehicle exhausts at the observation site in 2013.

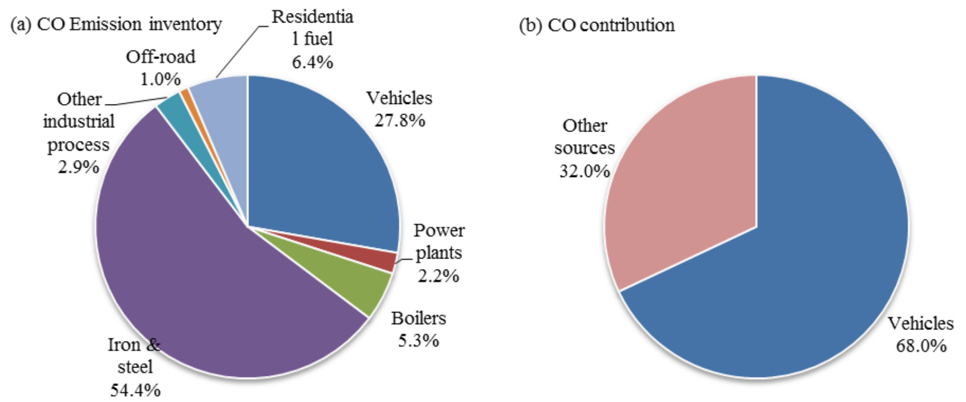

Fig. S5. CO emission contribution of different sources in the whole city (a) and contributions of vehicles and other sources to CO concentrations at the observation site in urban Shanghai (b).

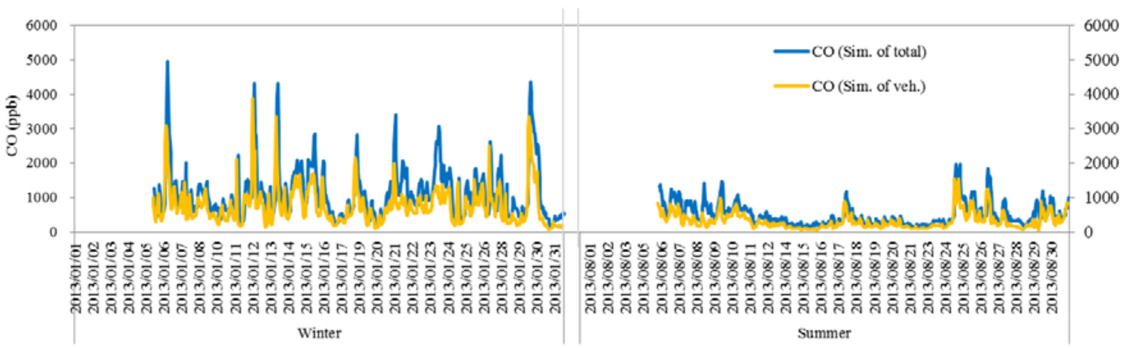

Fig. S6. Time series simulation data of CO concentration based on the CO emission inventories of the total emission sources and vehicle exhausts at the observation site in 2013.

References

Huang, C., Chen, C. H., Li, L., Cheng, Z., Wang, H. L., Huang, H. Y., Streets, D. G., Wang, Y. J., Zhang, G. F., and Chen, Y. R.: Emission inventory of anthropogenic air pollutants and VOC species in the Yangtze River Delta region, China, Atmos. Chem. Phys., 11, 4105–4120, doi:10.5194/acp-11-4105-2011, 2011.

Qiao, L. P., Cai, J., Wang, H. L., Wang, W. B., Zhou, M., Lou, S. R., Chen, R. J., Dai, H. X., Chen, C. H., Kan, H. D.: $PM_{2.5}$ constituents and hospital emergency-room visits in Shanghai, China, Environ. Sci. Technol, 48, 10406−10414, 2014.